Orientation and lateral mobility of cytochrome *c* on the surface of ultrathin lipid multilayer films

James M. Pachence,* Suzanne Amador,* Grzegorz Maniara,‡ Jane Vanderkooi,‡
P. Leslie Dutton,‡ and J. Kent Blasie*
*Department of Chemistry and ‡Department of Biochemistry and Biophysics, University of Pennsylvania, Philadelphia, Pennsylvania 19104 USA

ABSTRACT We have previously shown that cytochrome *c* can be electrostatically bound to an ultrathin multilayer film having a negatively charged hydrophilic surface; furthermore, x-ray diffraction and absorption spectroscopy techniques indicated that the cytochrome *c* was bound to the surface of these ultrathin multilayer films as a molecular monolayer. The ultrathin fatty acid multilayers were formed on alkylated glass, using the Langmuir-Blodgett method. In this study, optical linear dichroism was used to determine the average orientation of the heme group within cytochrome *c* relative to the multilayer surface plane. The cytochrome *c* was either electrostatically or covalently bound to the surface of an ultrathin multilayer film. Horse heart cytochrome *c* was electrostatically bound to the hydrophilic surface of fatty acid multilayer films having an odd number of monolayers. Ultrathin multilayer films having an even number of monolayers would not bind cytochrome *c*, as expected for such hydrophobic surfaces. Yeast cytochrome *c* was covalently bound to the surface of a multilayer film having an even number of fatty acid monolayers plus a surface monolayer of thioethyl stearate. After washing extensively with buffer, the multilayer films with either electrostatically or covalently bound cytochrome *c* were analyzed for bound protein by optical absorption spectroscopy; the orientation of the cytochrome *c* heme was then investigated via optical linear dichroism. Polarized optical absorption spectra were measured from 450 to 600 nm at angles of 0°, 30°, and 45° between the incident light beam and the normal to the surface plane of the multilayer. The dichroic ratio for the heme alpha-band at 550 nm as a function of incidence angle indicated that the heme of the electrostatically-bound monolayer of cytochrome *c* lies, on average, nearly parallel to the surface plane of the ultrathin multilayer. Similar results were obtained for the covalently-bound yeast cytochrome *c*. Furthermore, fluorescence recovery after photobleaching (FRAP) was used to characterize the lateral mobility of the electrostatically bound cytochrome *c* over the monolayer plane. The optical linear dichroism and these initial FRAP studies have indicated that cytochrome *c* electrostatically bound to a lipid surface maintains a well-defined orientation relative to the membrane surface while exhibiting measurable, but highly restricted, lateral motion in the plane of the surface.

INTRODUCTION

Membrane systems reconstituted from pure lipids and pure membrane proteins have proved to be valuable tools for establishing detailed information on the supramolecular organization of membrane systems such as those involved in biological electron transfer (e.g., photosynthesis, oxidative phosphorylation [1–5]). Such structural information, coupled with functional information from these reconstituted membrane systems (e.g., investigation of transmembrane phenomena) has lead to greater understanding of the cellular energy conversion process (6–8).

Recently, we have reconstituted a membrane system consisting of an ultrathin lipid multilayer film, formed via the Langmuir-Blodgett technique, possessing a surface molecular monolayer of cytochrome *c* (9, 10). Such systems, and other closely related complexes (such as inorganic multilayers possessing a surface monolayer of protein [11]), are ideally suited for detailed structural studies of specific membrane protein complexes with cytochrome *c* via x-ray diffraction and electron microscopy techniques (9–11). In addition, these tailored systems can be utilized for definitive functional studies on the electrochemistry and/or photochemistry of these membrane-protein complexes. The previous nonresonance x-ray diffraction studies of ultrathin lipid multilayer films with an electrostatically bound cytochrome *c* surface monolayer firmly established the position of the protein as a monolayer with respect to the lipid multilayer profile structure (9). In addition, resonance x-ray diffraction was utilized to determine directly the location of the heme iron atom within the profile structure of the cytochrome *c* monolayer on the surface of the ultrathin lipid film (10). The success of these initial structural studies using this reconstituted model system clearly established the viability of such protein surface monolayer/ultrathin lipid film systems to study the supramolecular organization of functional membrane-protein complexes.

In this study, optical linear dichroism was used to further determine the orientation of the heme group of cytochrome *c* bound to the surface of ultrathin lipid multilayer films. Various cytochrome *c*/lipid combinations were investigated; horse heart cytochrome *c* electrostatically bound to ultrathin lipid films having a surface

0006-3495/90/08/379/11 $2.00

monolayer of either arachidic acid or phosphatidylserine, or via polar interactions to a surface monolayer of thioethyl stearate. Alternatively, yeast cytochrome *c* was electrostatically bound to ultrathin lipid films having a surface monolayer of arachidic acid or phosphatidylserine, or covalently linked to a surface monolayer of thioethyl stearate (yeast cytochrome *c* has a cysteine residue located near the carboxy-terminus at sequence position 102, which forms a disulfide linkage spontaneously with the thiol moiety of the thioethyl stearate surface layer [12]). The orientation of the heme group of the bound cytochrome *c*, together with the previously derived structural information, provides unambiguously the orientation and position of the protein with respect to the surface of these ultrathin lipid films.

MATERIALS AND METHODS

Glass microscope slides cut to dimensions of 11 × 25 × 1 mm^3 were reacted with octadecyltrichlorosilane (OTS, Aldrich Chemical Co., Milwaukee, WI), according to the method by Sagiv (13) to form a hydrophobic substrate surface. Arachidic acid (Aldrich Chemical Co.) was zone refined with 50 zone passes at a rate of 1 cm/h and the purity of the center fraction confirmed by differential scanning calorimetric measurements (Dupont Co. 990, Wilmington, DE). Phosphatidylserine was purchased from Avanti Polar Lipids, Inc., Birmingham AL. Mercaptoethanol, methyl methane thiosulfonate, stearic acid, stearic anhydride, and pyridine were products of Aldrich Chemical Co. Type VI horse heart cytochrome *c* and yeast cytochrome *c* from *Saccharomyces cerevisiae* were obtained from Sigma Chemical Co., St. Louis, MO.

An analogue of a stearic acid possessing a sulfhydryl group in the polar headgroup was synthesized (thioethyl stearate; IPAC name: octadecanoic acid 2-mercaptoethyl ester; formula: $C_{20}H_{40}O_2S$). The procedure was essentially that of Ganong and Bell (14), with modifications to synthesize a thiol-fatty acid versus the phosphatidylthioglycerol of the original report (14). 5 mmol mercaptoethanol, 5.5 mmol methyl methanethiosulfonate, and 6 mmol pyridine were added to 10 ml chloroform in a nitrogen-flushed vessel, and reacted for 15 min. The resulting thiomethylthioethanol was purified by silica gel chromatography in chloroform, using a 1–15% gradient of methanol in 2% steps. Each fraction was analyzed using thin-layer chromatography (flexible plates [Eastman Kodak Co., Rochester, NY] cut to dimensions of 1 × 2 in) with a chloroform-methanol-water solvent (65:25:4 vol/vol). A control plate of mercaptoethanol, pyridine, and methyl methanethiosulfonate was run in parallel. The samples were visualized by exposure to iodine vapor. The R_f of the mercaptoethanol was ~0.18, thiomethylthioethanol was 0.30, pyridine was 0.65, and methyl methanethiosulfonate was 0.78. The appropriate fractions were pooled, then dried under nitrogen (yield was ~25 μmol).

1 ml of heptane was added to the dried thiomethylthioethanol, and dissolved; 2 ml $CHCl_3$, 125 μmol pyridine, and 60 μmol stearic anhydride were added; this combination was mixed, then allowed to react under N_2 for 24 h at room temperature in the dark. After evaporating the solvents, the residue was extracted with a chloroform/methanol/0.1 N HCl solution as described by Bligh and Dyer (15). The lower chloroform phase was dried down under N_2, and the reactants were separated using thin-layer chromatography (2-mm-thickness plate [Eastman Kodak Co.] with a heptane/diethyl ether/acetic acid solvent, 25:75:1 vol/vol). A control plate of methyl methanethioethanol, stearic anhydride, and stearic acid was run in parallel. The samples were visualized by ultraviolet light, and the material with an R_f of 0.7 was collected. The thiomethyl-thioethyl stearate was eluted with chloroform, then stored with N_2 at −20°C until used for deposition.

Multilayer lipid films (arachidic acid, thiomethyl-thioethyl stearate, and phosphatidylserine) were deposited onto the alkylated glass substrates via the Langmuir-Blodgett technique, as described previously (9). A subphase consisting of 1 mM $BaCl_2$, 0.1 mM $NaHPO_3$ was first bubbled with N_2 to remove O_2, brought to pH = 9.0 ± 0.2, then was placed in a Lauda Langmuir trough system; the lipid monolayer was kept at a constant surface pressure of 20 dyn/cm and a temperature of 17.5°C during the deposition, with the pH monitored during deposition (pH = 8.5 ± 0.5). The substrate was passed through the monolayer at a rate of 0.3 cm/min. Four monolayers of arachidate were deposited onto each substrate; a final surface layer consisting of arachidic acid, thiomethyl-thioethyl stearate, or phosphatidylserine was then deposited (with the subphase surface being cleaned before the formation of the thiomethyl-thioethyl stearate or phosphatidylserine monolayers). In each case, an odd number of monolayers was deposited, and therefore a 10-ml glass vial was placed in the subphase directly below the dipping mechanism before forming the lipid monolayer on the subphase. The glass slide, being below the subphase on the deposition of the last of an odd number of monolayers, was released from the dipping mechanism directly into the glass vial. In this manner, the final hydrophilic film surface was always thereafter in contact with the polar solvent. The glass vial was then placed into a 500-ml container of buffer (1 mM $NaHCO_3$ at pH 8) and allowed to equilibrate for 24 h. The barium-free buffer was changed twice over the next 24-h period.

The multilayer films containing a surface monolayer of thiomethyl-thioethyl stearate (TTS) was activated before use by removing the thiomethyl group, forming thioethyl stearate (TES). This was done by placing the glass slide substrate into a glass vial containing the 1 mM $NaHCO_3$, pH 8.0 ± 0.2, and 0.1 mM dithiothreitol for 1 h. The supernatant was then replaced with 1 mM $NaHCO_3$, pH 8.0 ± 0.2 three times before reacting these films with cytochrome *c*.

Ultrathin multilayer films consisting of five lipid monolayers (with surface monolayers of arachidic acid, thioethyl stearate, or phosphatidylserine) were incubated for 48 h or more in 10 μM yeast or horse heart cytochrome *c* solution in 1 mM $NaHCO_3$, pH 8. Each film was removed from the cytochrome *c* solution, and incubated with 1 mM $NaHCO_3$ buffer for 2 h or more. The buffer was changed every 5 min until there was no detectable cytochrome *c*, measured spectrophotometrically in the supernatant. The glass slide substrate supporting the ultrathin multilayer films was then suspended in a quartz cuvette (1 cm path length), containing a solution of 1 mM $NaHCO_3$ and between 0.01 and 0.1 mM ascorbate (to reduce the cytochrome *c*) at pH 8, and the optical absorption spectra were recorded with a double-beam spectrophotometer (9).

Spectra for the linear dichroism measurements were recorded using a computer-driven scanning dual-beam apparatus (Johnson Foundation, University of Pennsylvania) having a maximal range of 400 to 1,200 nm. The linear dichroism measurements were recorded over a range of 450 to 610 nm, with the reference wavelength set at 600 nm. Polarization was accomplished by using a Nicole prism (Oriel Corp., Stamford, CT); light is polarized either horizontally (perpendicular to the axis of sample rotation) or vertically (parallel to the axis of sample rotation). The dichroic ratio was calculated as the absorption with horizontally polarized light divided by the absorption with vertically polarized light at a particular wavelength and angle of incidence (the angle of rotation between the measuring beam and the normal to the plane of the multilayer film, which could be varied by 15° intervals). The cuvette that was used to orient the sample relative to the incident light is described elsewhere (16). Data was collected using an IBM PC, and was analyzed using the ASYSTANT + program (MacMillan Software Co., New York).

RESULTS

Fig. 1 *A* shows a typical optical absorption spectrum (wavelength range, 350–500 nm) from a three-monolayer arachidic acid film (having a hydrophilic surface), preincubated with yeast cytochrome *c* as outlined in Methods, exhibiting a typical Soret band for reduced cytochrome *c*. By comparing Fig. 1 *A* with spectra measured previously on various arachidic acid/cytochrome *c* films (9), it was determined that the optical density at 410 nm of Fig. 1 *A* is approximately equal to that for a hexagonally close packed monolayer of cytochrome *c* bound to the arachidic acid surface. As the interaction between yeast cytochrome *c* and the arachidic acid surface should be mainly electrostatic, binding should therefore be inhibited at high ionic strength. Therefore, the arachidic acid multilayer films with bound yeast cytochrome *c* were then incubated with 0.1 M NaCl for 24 h or more. The optical absorption spectrum from the glass slide with these multilayer films (reduced with ascorbate) were subsequently measured (as shown, for example, in Fig. 1 *B*). Less than half (~35%) of the optical absorbance from yeast cytochrome *c* remained on the multilayer film; conversely, it was found that the remaining yeast cytochrome *c* could be accounted for in the supernatant which was used to treat the multilayer film at high ionic strength. It was previously shown that horse heart cytochrome *c* similarly exhibited primarily electrostatic binding to hydrophilic surfaces of ultrathin multilayer films of arachidic acid (9); <10% of the cytochrome *c* remained bound after treatment of the multilayer film at high ionic strength. No detectable cytochrome *c* spectra were observed when either horse heart or yeast cytochrome *c* solutions were incubated with arachidic acid ultrathin multilayer films have hydrophobic surfaces (four or six monolayers of arachidic acid).

In a similar fashion, a yeast cytochrome *c* solution was incubated with an ultrathin multilayer film having four monolayers of arachidic acid (AA) and a surface monolayer of phosphatidylserine (PS). As described above, the optical absorption spectra from this AA-PS film preincubated with yeast cytochrome *c* shows a typical Soret band for reduced cytochrome *c* (Fig. 2 *A*). The optical density at 410 nm of Figs. 1 *A* and 2 *A* are comparable; therefore, the optical density at 410 nm of Fig. 2 *A* is also approximately equal to that for a hexagonally close packed cytochrome *c* monolayer bound to the lipid film surface. Similarly, the AA-PS multilayer films with bound yeast cytochrome *c* were then incubated with 0.1 M NaCl for 24 h or more. The optical spectra from the glass slide with these multilayer films (reduced with ascorbate) were subsequently measured, as shown in Fig. 2 *B*. In this case, most of the optical absorbance from yeast cytochrome *c* remained on the AA-PS multilayer film (as compared to Fig. 1 *B* for the AA multilayer film). Higher concentrations of NaCl (up to 2 M), and longer time periods of incubation with a high ionic strength solution, did not remove the yeast cytochrome *c* from the AA-PS multilayer film. However, treatment of these AA-PS multilayer films possessing a bound surface monolayer of yeast cytochrome *c* with a 0.1 mM solution of dithiothreitol (1 mM $NaHCO_3$, pH 8.0) did remove more than 85% of the yeast cytochrome *c* into the supernatant (data not shown). As before, horse heart cytochrome *c* exhibited primarily electrostatic binding to hydrophilic surfaces of these AA-PS multilayer films (data not shown).

Lastly, a multilayer film consisting of four monolayers of arachidic acid and a surface monolayer of thiomethylthioethyl stearate (TTS) was prepared; the protecting thiomethyl group was removed to form thioethyl stearate (TES) before incubating the multilayer film with a yeast cytochrome *c* solution. As described above, the optical

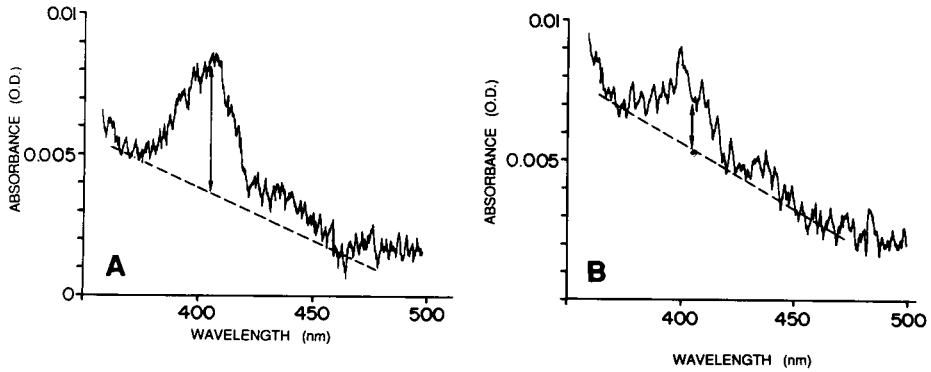

FIGURE 1 Optical absorption spectra: (*A*) yeast cytochrome *c* bound to the surface of an ultrathin multilayer substrate consisting of three monolayers of arachidic acid; (*B*) the ultrathin film of *A* after treatment with 100 mM KCl (48 h), which was then placed in fresh buffer. As was shown previously, the 100 mM KCl supernatant from *B* contained the released cytochrome *c* (9).

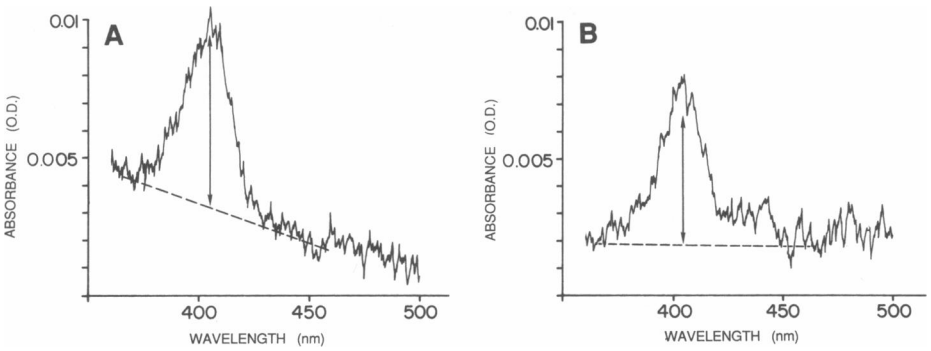

FIGURE 2 Optical absorption spectra (*A*) yeast cytochrome *c* bound to the surface of an ultrathin multilayer substrate consisting of four monolayers of arachidic acid and one monolayer of phosphatidylserine; (*B*) the ultrathin film of *A* after treatment with 100 mM KCl (>48 h).

absorption spectra from these AA-TES films preincubated with yeast cytochrome *c* exhibit a typical Soret band for reduced cytochrome *c* (Fig. 3 *A*). Again, the optical density at 410 nm of Figs. 1 *A*, 2 *A* and 3 *A* are comparable; therefore, the optical density at 410 nm of Fig. 3 *A* is also approximately equal to that for a hexagonally close packed cytochrome *c* monolayer bound to the lipid film surface. The AA-TES multilayer film with bound yeast cytochrome *c* were then incubated with 0.1 m NaCl for 24 h or more. The optical spectrum from the glass slide with these multilayer films (reduced with ascorbate) was subsequently measured, as shown in Fig. 3 *B*. Similar to the AA-PS multilayer films (Fig. 2 *B*), most of the optical absorbance from yeast cytochrome *c* remained on the AA-TES multilayer film (as compared to Fig. 1 *B* for the AA multilayer film). Higher concentrations of NaCl (up to 2 M) and longer time periods of incubation with a high–ionic strength solution did not remove the yeast cytochrome *c* from the AA-TES multilayer film. Yeast cytochrome *c* was removed from the AA-TES multilayer surface by treating the film with a strong reducing agent such as dithiothreitol. Horse heart cytochrome *c* exhibited binding via primarily polar interactions to the hydrophilic surface of the AA-TES multilayer film because high salt concentrations again removed the cytochrome *c* from lipid surface (data not shown).

Polarized optical absorption spectra (wavelength range, 450–600 nm) for the ultrathin multilayer films having a bound surface monolayer of cytochrome *c* were measured. Fig. 4 shows typical optical absorption spectra for an ultrathin multilayer film of three monolayers of arachidic acid with a bound surface monolayer of yeast cytochrome *c* for horizontal and vertical polarizations at three angles of incidence; this wavelength range was chosen to show the alpha and beta absorption bands of cytochrome *c*. The angle of incidence α is defined as the angle of rotation between the incident beam and the *z*-axis normal to the plane of the mutilayer; the vertical (horizontal) polarization is parallel (perpendicular) to the axis of rotation. The optical absorption spectra in this region for horizontal and vertical polarizations (*A* and *B*, respectively) are nearly identical for 0° angle of incidence, which is expected for a chromophore that is isotropically oriented within the surface plane. As can be seen by comparing the horizon-

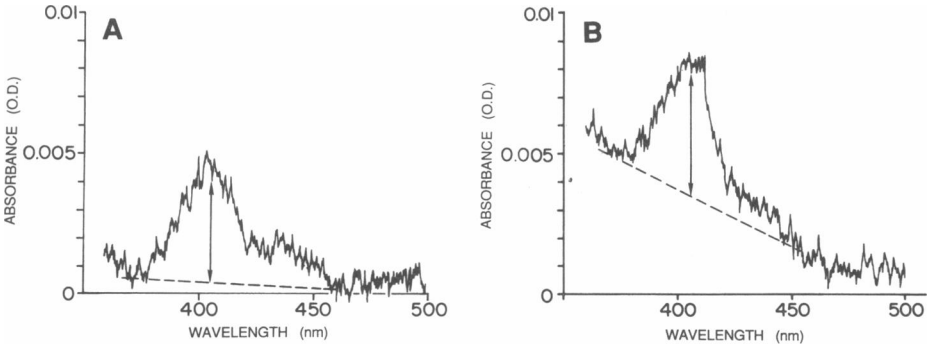

FIGURE 3 Optical absorption spectra (*A*) yeast cytochrome *c* bound to the surface of an ultrathin multilayer substrate consisting of four monolayers of arachidic acid and one monolayer of the thioethyl stearate; (*B*) the ultrathin film of *A* after treatment with 100 mM KCl (>48 h).

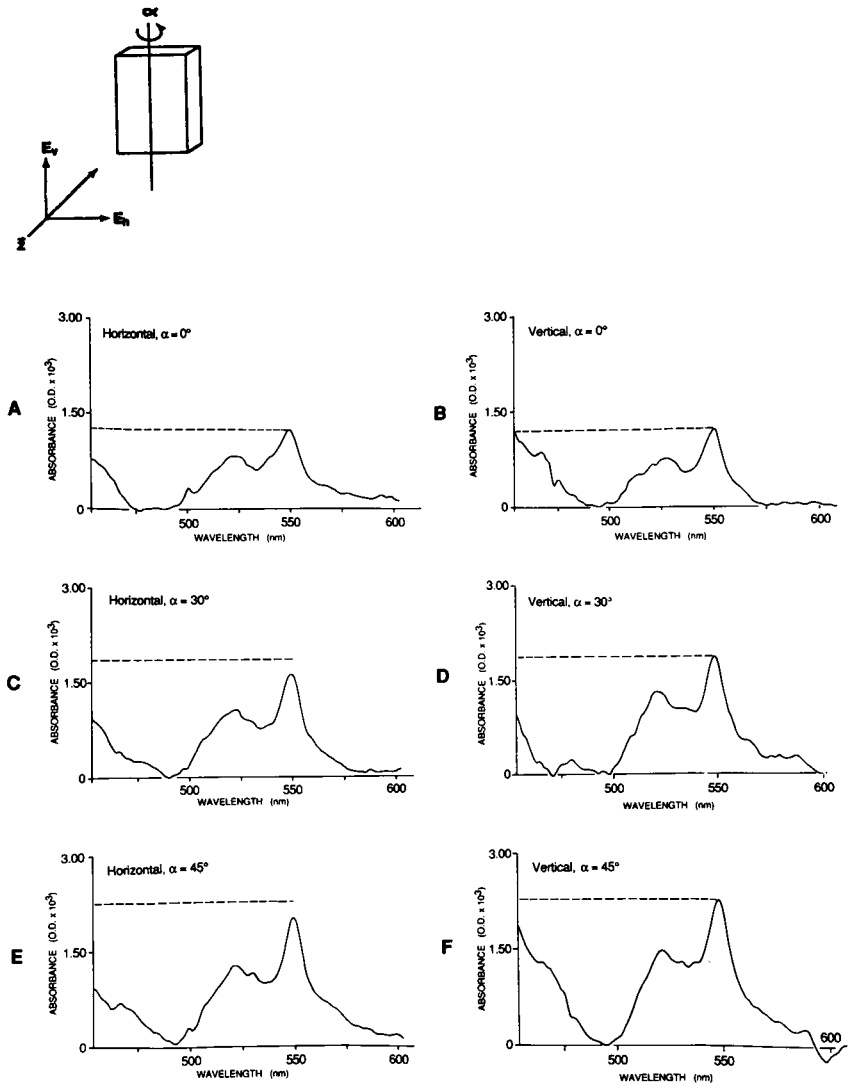

FIGURE 4 Polarized optical absorption spectra for an ultrathin multilayer film of three monolayers of arachidic acid with a bound surface monolayer of yeast cytochrome *c*. The ultrathin multilayer film with bound cytochrome *c* was immersed in 1 mM $NaHCO_3$, 60% glycerol, pH 7.5 solution at room temperature during the experiment. The angle of incidence α is defined as the angle of rotation between the incident beam and the *z*-axis normal to the plane of the multilayer; the vertical (horizontal) polarization is parallel (perpendicular) to the axis of rotation. (*A*) $\alpha = 0°$, (*C*) $\alpha = 30°$, and (*E*) $\alpha = 45°$ at horizontal polarization; (*B*) $\alpha = 0°$, (*D*) $\alpha = 30°$, and (*F*) $\alpha = 45°$ at vertical polarization. Noise was reduced by subjecting the data to five-channel smoothing.

tally versus vertically polarized absorption spectra for $\alpha = 30°$ and 45° angles of incidence (*C* and *D*, *E* and *F*), the optical density from the heme at 520 and 550 nm (beta- and alpha-bands, respectively) are no longer identical for these polarizations. Similar polarized optical absorption spectra were collected for yeast and horse heart cytochrome *c* to AA-PS AA-TES multilayer films. Polarized optical absorption spectra of OTS-treated glass substrates and of ultrathin multilayer films without cytochrome *c* were recorded before every experiment to insure that the dichroic effects observed for the cytochrome *c* monolayer with $\alpha > 1°$ were due exclusively to cytochrome *c*.

To more readily observe the changes in the optical absorption spectra for the two polarizations for each of the cytochrome *c*/lipid multilayer combinations, we generated difference-polarized optical absorption spectra (horizontal minus vertical polarization. The difference-polarized optical absorption spectra for an AA ultrathin multilayer film with a bound monolayer of yeast cytochrome *c*, for angles of incidence 0, 30, and 45° are shown, for example, in Fig. 5. Similarly, the difference-

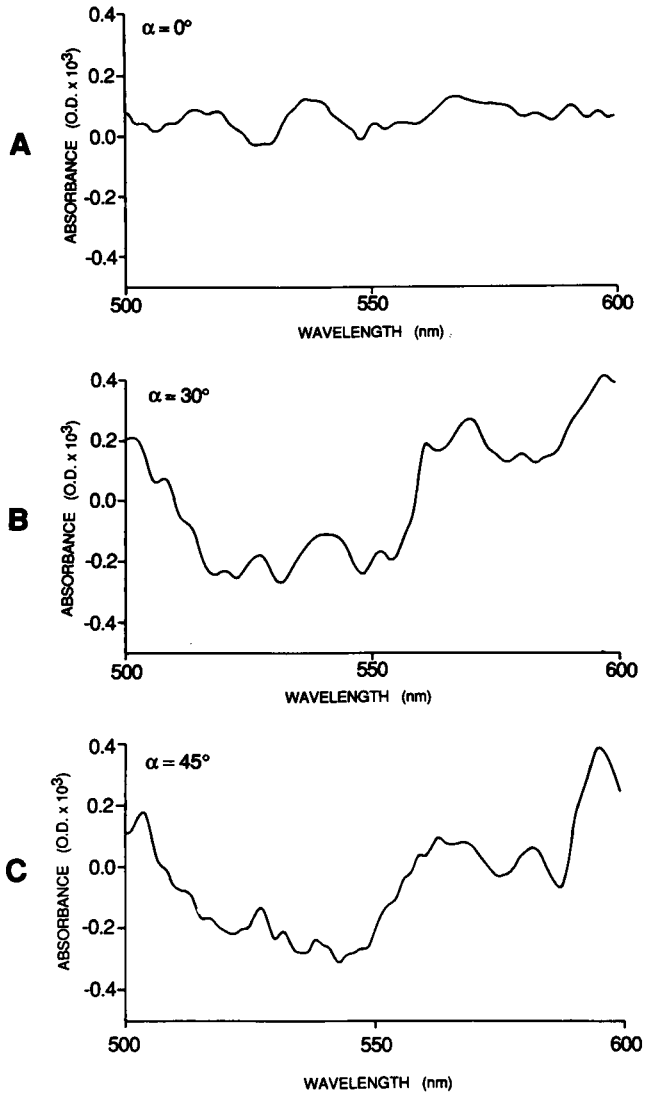

FIGURE 5 Difference-polarized optical absorption spectra (horizontal minus vertical polarization) for an ultrathin multilayer film of three monolayers of arachidic acid with a bound surface monolayer of yeast cytochrome *c*, for angles of incidence: (*A*) $\alpha = 0°$ (Fig. 4 *A* minus 4 *B*), (*B*) $\alpha = 30°$ (Fig. 4 *C* minus 4 *D*), and (*C*) $\alpha = 45°$ (Fig. 4 *E* minus 4 *F*). Noise was reduced by subjecting the data to five-channel smoothing.

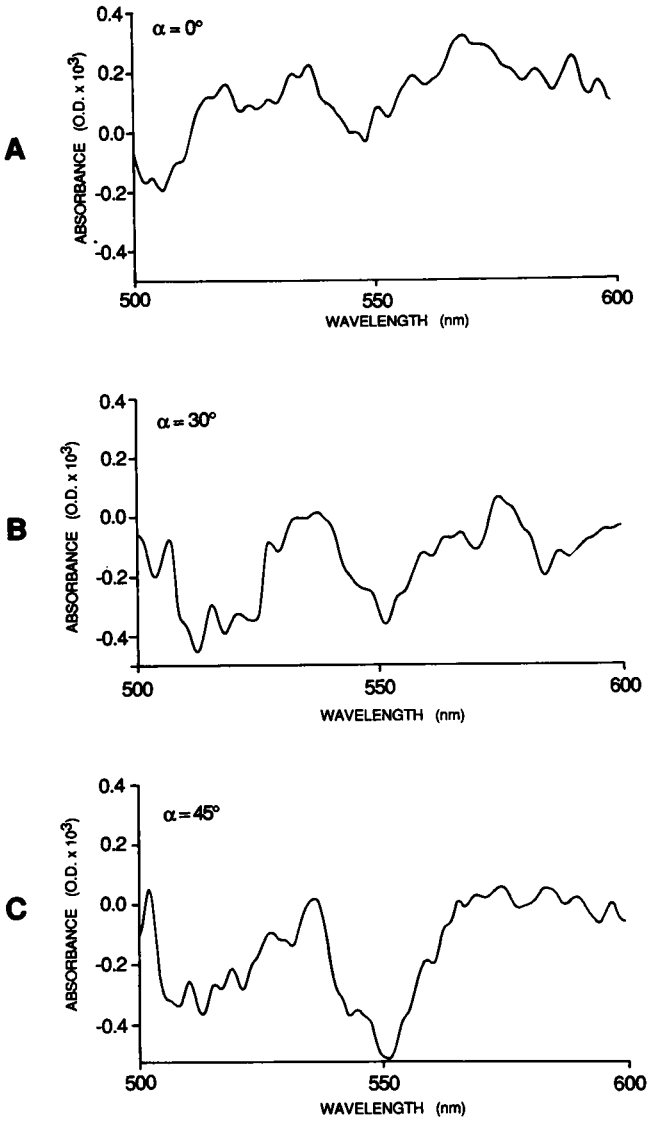

FIGURE 6 Difference-polarized optical absorption spectra (horizontal minus vertical polarization) for an ultrathin multilayer film of four monolayers of arachidic acid and one monolayer of phosphatidylserine, with a bound surface monolayer of yeast cytochrome *c*, for angles of incidence: (*A*) $\alpha = 0°$, (*B*) $\alpha = 30°$, and (*C*) $\alpha = 45°$. Noise was reduced by subjecting the data to five-channel smoothing.

polarized optical absorption spectra for typical AA-PS ultrathin multilayer films with a bound surface monolayer of yeast cytochrome *c* and the AA-TES with a bound monolayer of yeast cytochrome *c* are shown in Figs. 6 and 7, respectively. An equivalent series of difference-polarized optical absorption spectra were generated for horse heart cytochrome *c* bound to AA, AA-PS, and AA-TES multilayer films (data not shown). As can be seen in Figs. 5–7, showing the difference-polarized spectra of the heme beta- and alpha-bands at 520 and 550 nm, respectively, the horizontally-polarized optical density decreases in general relative to the vertically-polarized optical density with increasing angle of incidence; this can be seen by comparing the polarized absorption spectra themselves, as in Fig. 4. Hence, the difference-polarized optical absorption spectra of Figs. 5–7 have increasingly negative values as a function of increasing angle of incidence, starting from approximately zero OD at 0°. These changes with angle of incidence are readily apparent and reproducible (multilayer to multilayer) in spite of

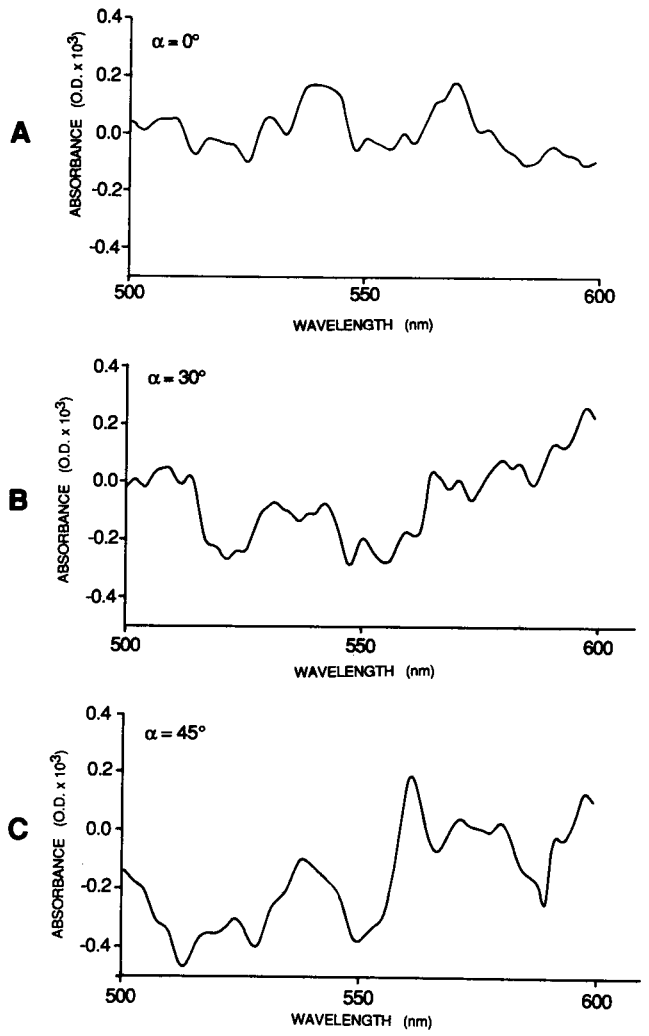

FIGURE 7 Difference-polarized optical absorption spectra (horizontal minus vertical polarization) for an ultrathin multilayer film of four monolayers of arachidic acid and one monolayer of the thioethyl stearate with a bound surface monolayer of cytochrome *c*, for angles of incidence: (*A*) $\alpha = 0°$, (*B*) $\alpha = 30°$, and (*C*) $\alpha = 45°$. Noise was reduced by subjecting the data to five-channel smoothing.

the relatively low signal-to-noise level in the polarized optical spectra from these cytochrome *c* monolayers bound to lipid surfaces. The most pronounced difference optical densities are in general exhibited for the characteristics absorption maxima for cytochrome *c* at 520 and 550 nm, respectively, over this spectral region. The dichroic ratios were measured directly from the polarized optical absorption spectra for each cytochrome *c*/lipid multilayer combination at 520 and 550 nm as shown in Table 1.

Finally, initial fluorescence recovery after photobleaching (FRAP) experiments were performed to determine the extent of lateral mobility of the cytochrome *c* on the multilayer surface. An ultrathin multilayer film consisting of three monolayers of arachidic acid with an electrostatically-bound surface monolayer of porphyrin cytochrome *c* was used (porphyrin cytochrome *c* exhibits the high degree of fluorescence necessary for the FRAP experiment [17]). The ultrathin multilayer film with porphyrin cytochrome *c* was immersed in a 1 mM $NaHCO_3$, pH 7.5 buffer during the FRAP experiment. The actual data in Fig. 8 are shown as points, and the solid lines are the best fits to the data (17). At a sample temperature of 22.5°C, the lateral diffusion coefficient for porphyrin cytochrome *c* was determined to be $D = 4.23 \pm 0.33 \times 10^{-10}$ cm²/s. At a sample temperature of 12°C, the lateral diffusion coefficient for the porphyrin cytochrome *c* was determined to be $D = 0.57 \pm 0.21 \times 10^{-10}$ cm²/s. The diffusion coefficient for cytochrome *c* in solution at 22.5°C was at least two orders of magnitude faster than for the electrostatically-bound protein (data not shown).

TABLE 1 **Dichroic ratio: $A_{horizontal}/A_{vertical}$**

Angle of incidence	OD_{520}	OD_{550}	Sample
degrees			
0	1.04	1.00	
30	0.81	0.86	3 × AA,
45	0.82	0.80	HH cyt *c*
0	1.14	1.00	
30	0.72	0.82	3 × AA,
45	0.82	0.80	Yeast cyt *c*
0	1.02	1.05	
30	0.91	0.96	4 × AA, PS,
45	0.82	0.82	HH cyt *c*
0	1.07	1.00	
30	0.91	0.87	4 × AA, PS,
45	0.95	0.84	Yeast cyt *c*
0	1.10	1.01	
30	0.91	0.91	4 × AA, TES,
45	0.75	0.80	HH cyt *c*
0	1.00	1.02	
30	0.88	0.91	4 × AA, TES,
45	0.80	0.79	Yeast cyt *c*

AA, arachidic acid (Example: 3 × AA = three monolayers of arachidic acid); HH, cytochrome *c* from horse heart; PS, phosphatidylserine; TES, thiolethyl stearic acid.

DISCUSSION

Previous studies showed that the binding of horse heart cytochrome *c* onto ultrathin lipid multilayer films having a hydrophilic surface was primarily electrostatic (9).

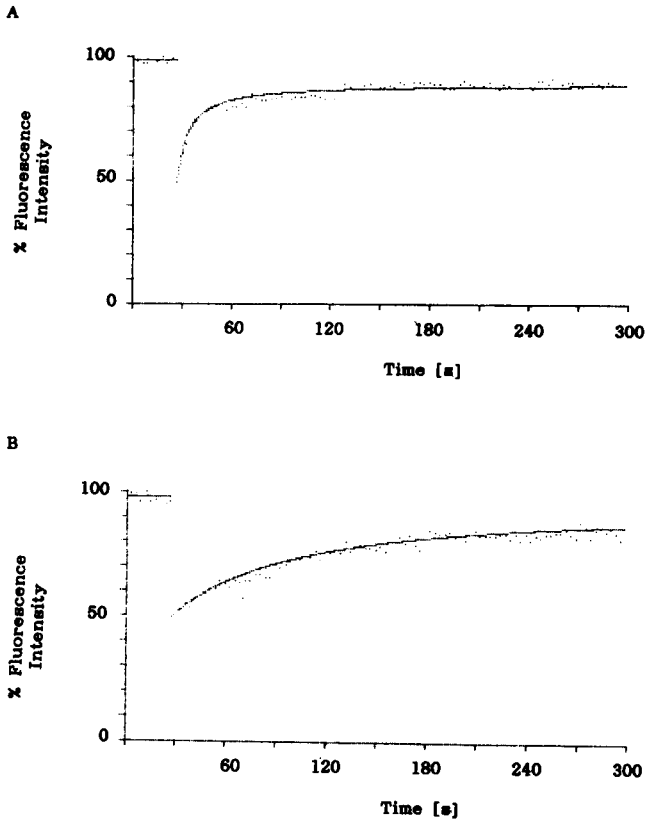

FIGURE 8 FRAP, shown as a percentage of the initial fluorescence value as a function of time, for an ultrathin multilayer film of three monolayers of arachidic acid with an electrostatically-bound surface monolayer of porphyrin cytochrome *c*. The ultrathin multilayer film with porphyrin cytochrome *c*, which was deposited onto an alkylated glass substrate via the Langmuir-Blodgett technique, was immersed in a 1 mM $NaHCO_3$, pH 7.5 buffer during the FRAP experiment. The actual data are shown as points, and the solid line is the best fit to the data, using the method of Vanderkooi et al. (25). (*A*) At a sample temperature of 22.5°C, the lateral diffusion coefficient for porphyrin cytochrome *c* was determined to be $D = 4.23 \pm 0.33 \times 10^{-10}\ cm^2/s$; (*B*) At a sample temperature of 12°C, $D = 0.57 \pm 0.21 \times 10^{-10}\ cm^2/s$.

Therefore, it was not surprising to find in the present study that yeast cytochrome *c* binding to an ultrathin arachidic acid film having a hydrophilic surface is primarily electrostatic. It was also not surprising that the yeast cytochrome *c* binds covalently to the thioethyl stearate surface, given that it had been previously reported that yeast cytochrome *c* binds covalently to extrinsic thiol groups through a cysteine residue located in the carboxyl-terminal alpha helix, accessible to its surface (18). Conversely, horse heart cytochrome *c* does not have a surface cysteine residue, and did not bind covalently to the thiol derivative fatty acid surface, as expected.

However, it was surprising that the binding of yeast cytochrome *c* to the phosphatidylserine surface was covalent. Similar to disulfide linkage with the thioethyl stearate surface, yeast cytochrome *c* was removed from the phosphatidylserine surface only with strong reduction. One explanation for this result is that the thiol group of the yeast cytochrome *c* cysteine residue 102 reacted with the amino group of the phosphatidylserine; it has been shown that thiol-amino reactions occur spontaneously in the presence of oxygen. Indeed, a preliminary experiment was done to show that this reaction can be inhibited. When yeast cytochrome *c* was reacted with the AA-PS multilayer film under an N_2 atmosphere, >60% of the cytochrome *c* was subsequently removed from the surface when the cytochrome/AA-PS film was incubated with 250 mM KCl.

It should be noted that the characteristic shapes of the background optical spectra in Figs. 1–3 varied; this variation in the local background in the vicinity of the Soret band can be attributed to variations in the reference sample (e.g., variations in the glass slide substrates).

The pi-pi* optical transitions of the cytochrome *c* heme responsible for the absorption maxima at 520 and 550 nm are *x-y* polarized in the plane of the heme ring (17); the orientation of the heme plane of cytochrome *c* with respect to the monolayer surface plane can therefore be determined (19). Qualitatively, the heme plane of the cytochrome *c* would be approximately parallel to the monolayer surface if the horizontally polarized optical density decreases relative to the vertically polarized optical density with increasing angle of incidence (as the couplings of the horizontal polarization vector with the in-plane heme transitions are decreasing at the angle of incidence between the monolayer surface plane and the horizontal polarization vector increases from 0°); conversely, the horizontally-polarized optical density increases relative to the vertically polarized optical density with increasing angle of incidence if the heme is perpendicular to the monolayer surface (19). In both cases, the coupling of the vertical polarization vector with these heme transitions remains constant as a function of angle of incidence. A quantitative treatment of the dependence of the optical absorbance of linearly polarized light by heme groups within oriented multilayers on the angle of incidence can be found in reference 20. The dichroic ratios of both absorption maxima as listed in Table 1 tend to decrease as a function of increasing angle of incidence, indicating that the average orientation of cytochrome *c* heme groups was parallel to monolayer surface plane. The fact that the dichroic ratios reported are not decreasing as rapidly with increasing rotation angle as expected for an ensemble of heme groups which are precisely oriented parallel to the monolayer plane (whose mosaic spread or average layer misorientation is <0.01°) suggests some finite distribution of heme plane orientations about the mean value parallel to the monolayer plane (20). Calcula-

tions in reference 20 would indicate that there is a rather broad distribution about the mean; however, the low signal-to-noise level of these dichroism measurements on such heme protein single monolayers also contributes to the apparently broad distribution of heme positions about the mean (it should be noted that the spectra of Figs. 4–7 are all subjected to five-channel smoothing).

The previous nonresonance x-ray diffraction studies of ultrathin lipid multilayer films with electrostatically bound cytochrome *c* established the position of the protein with respect to the surface of the lipid film (9). The results from these nonresonance x-ray diffraction studies revealed that the major axis of the cytochrome *c* prolate ellipsoid was parallel to the surface of the multilayer film (i.e., the cytochrome *c* monolayer plane). In addition, resonance x-ray diffraction studies were utilized to determine directly the location of the heme iron atom within the profile structure of the cytochrome *c* monolayer on the surface of the ultrathin lipid film to ±3 Å (10); using these methods, it was found that the heme-Fe atom was located near the center of the cytochrome *c* electron density profile (21). Hence, the results from both the x-ray diffraction experiments and the optical linear dichroism studies are fully consistent, requiring that the major axis of the cytochrome *c* ellipsoid be oriented parallel to the monolayer plane with the plane of the heme group also parallel to the monolayer plane. Furthermore, the nearly central location of the heme-Fe atom with respect to the three-dimensional electron density distribution of cytochrome *c* (12, 21), coupled with the resonance diffraction results which restrict the heme Fe location of ±3 Å within the monolayer profile, would allow such a broad distribution of heme orientations about the mean with respect to the monolayer surface (as indicated by the optical linear dichroism results presented in this paper [10]).

To further characterize the nature of the electrostatically-bound cytochrome *c* relative to the multilayer film surface, FRAP was used to determine the lateral mobility of cytochrome *c* over the surface (Fig. 8). The optical linear dichroism and FRAP studies indicate that although cytochrome *c* electrostatically bound to a lipid multilayer

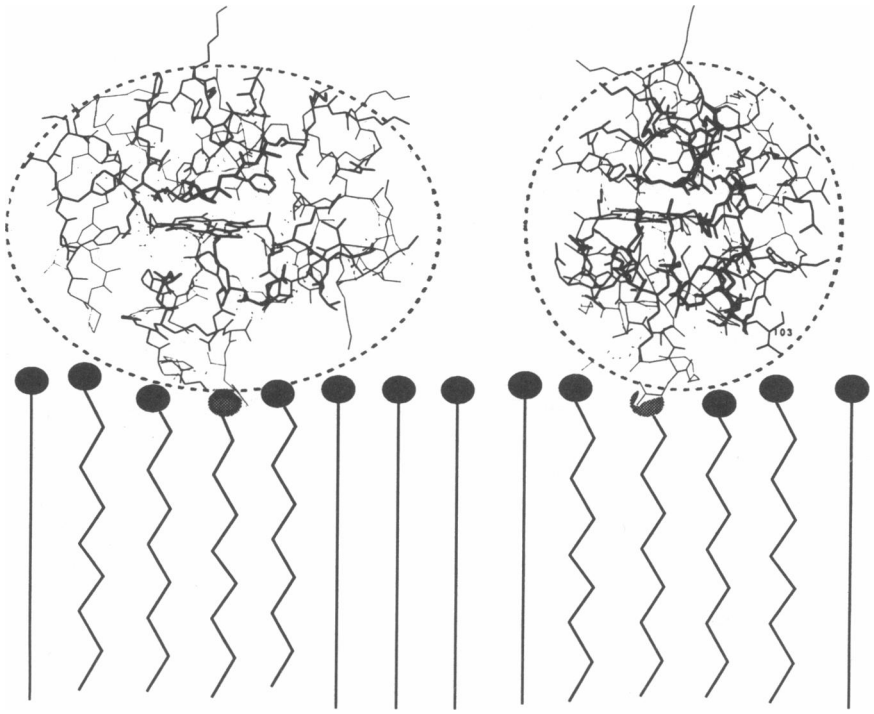

FIGURE 9 A schematic representation of an ultrathin multilayer film showing the surface monolayer of fatty acid with a bound monolayer of cytochrome *c*, indicating the structural information obtained from resonance and nonresonance x-ray diffraction, as well as optical linear dichroism. The previous x-ray diffraction results (reference 9) showed that the surface lipid monolayer was disordered (the lipid polar headgroups were less localized in the monolayer profile) as compared to the underlying monolayers, and that the cytochrome *c* molecules profile penetrate into the hydrophilic lipid carboxyl group layer (see Fig. 8 of reference 9). In this figure, the cytochrome *c* heme plane is shown as oriented parallel with respect to the membrane plane; this orientation represents the average orientation of a rather broad distribution as based on the optical linear dichroism results. Cytochrome *c* is rotationally averaged about the normal to the membrane surface; two representative orientations about the membrane normal were chosen to emphasize certain important structural features of the cytochrome *c*/lipid interaction.

surface of fixed negative charges exhibits measurable, but restricted, lateral mobility in the plane of the surface, its heme orientation is not as a result rotationally averaged with respect to the axes in the surface plane.

Fig. 9 summarizes pictorally the compiled structural information on the cytochrome *c*/ultrathin lipid multilayer films with the protein represented at atomic resolution (9–11). The structure of tuna cytochrome *c* was used for this figure which is virtually isomorphous with horse heart and yeast cytochromes *c* (21). It should be noted that the cytochrome *c* molecules are rotationally averaged about an axis perpendicular to the monolayer surface plane, which precludes the possibility of obtaining information on heme orientation within the monolayer surface plane (20) and that the orientation of the heme plane with respect to the surface plane represents only the average orientation of a rather broad distribution; two representative orientations about axes perpendicular to the monolayer plane were chosen to emphasize certain important structural features of the cytochrome *c*/lipid interaction. As can be seen in Fig. 9, the derived average orientation of cytochrome *c* can place residue 103 near the surface of the monolayer, which would also place the cysteine residue 102 of yeast cytochrome *c* near the surface of the lipid monolayer, thereby consistent with the covalent binding of residue 102 to the surface thiol residue of TES. It is presumably the nonelectrostatic, polar interactions which establish this average orientation of yeast cytochrome *c* on the TES monolayer surface, given the similar orientation of horse heart cytochrome *c* on the TES monolayer surface and the absence of purely electrostatic interactions for these two cases. These polar interactions between the two cytochrome *c*'s with the ester moiety of TES clearly facilitate the covalent binding of yeast cytochrome *c* to TES.

The heme orientation in the case of horse heart cytochrome *c* is, however, presumably determined mostly by electrostatic interactions between the acidic fatty acid surface and the basic residues on the cytochrome *c*, so our results may seem surprising in the light of previously published speculations on the structures of cytochrome *c*/protein ligand complexes which show the cytochrome *c* heme plane orientation perpendicular to the protein–protein interface (e.g., reference 22). However, these structures were assembled by assuming that the docking occurred between basic residues (principally lysines) fringing the cytochrome *c* heme crevice opening and negatively charged groups on the surface of the "receptor" protein (e.g., reference 23). Upon examination of the structure of tuna cytochrome *c*, it can be found that the basic residues lysine and arginine are fairly uniformly distributed over the surface of the protein. In the one study to date in which the full 6D configurational space of cytochrome *c*/cytochrome *c* peroxidase complex was explored, Warwicker found that "cytochrome *c* can interact favorably with cytochrome *c* peroxidase . . . over most of its surface" (23). Consequently, it is possible that either short-range interactions serve to fully determine only one configuration from many electrostatically-favored possibilities or that a variety of configurations close in free energy exist in an ensemble of such bimolecular complexes. Our results may be more consistent with the latter case. In fact, transitions within a distribution of cytochrome *c* orientations on membrane surfaces may be necessary to provide for electron transport with the integral membrane electron transfer proteins (24).

REFERENCES

1. Pachence, J. M., P. L. Dutton, and J. K. Blasie. 1979. Structural studies on reconstituted reaction center-lipid membranes. *Biochim. Biophys. Acta.* 548:348–373.
2. Pachence, J. M., P. L. Dutton, and J. K. Blasie. 1983. A structural investigation of cytochrome *c* binding to photosynthetic reaction centers in reconstituted membranes. *Biochim. Biophys. Acta.* 724:6–19.
3. Pachence, J. M., P. L. Dutton, and J. K. Blasie. 1981. The reaction center profile structure derived from neutron diffraction. *Biochim. Biophys. Acta.* 635:267–283.
4. Blasie, J. K., M. Erecinska, S. Samuels, and J. S. Leigh. 1978. The structure of a cytochrome oxidase-lipid model membrane. *Biochim. Biophys. Acta.* 501:33–53.
5. Henderson, R., and P. N. T. Unwin. 1975. Three-dimensional model of purple membrane obtained by electron microscopy. *Nature (Lond.).* 257:28–32.
6. Wikstrom, M., K. Krab, and M. Saraste. 1981. Proton translocating cytochrome complexes. *Annu. Rev. Biochem.* 50:623–655.
7. Lanyi, J. K. 1986. Halorhodopsin: a light-driven chloride ion pump. *Annu. Rev. Biophys. Biophys. Chem.* 15:11–28.
8. Villegas, R., G. M. Villegas, J. M. Rodriguez-Grille, and F. Sorais-Landez. 1988. The sodium channel of excitable and non-excitable cells. *Q. Rev. Biophys.* 21:99–128.
9. Pachence, J. M., and J. K. Blasie. 1988. The location of cytochrome *c* on the surface of ultrathin lipid multilayer films using x-ray diffraction. *Biophys. J.* 52:735–747.
10. Pachence, J. M., R. Fischetti, and J. K. Blasie. 1989. Location of the heme-Fe atoms within the profile structure of a monolayer of cytochrome *c* bound to the surface of an ultrathin lipid multilayer film. *Biophys. J.* 56:327–337.
11. Amador, S., J. M. Pachence, and J. K. Blasie. 1989. X-ray studies of cytochrome c monolayers bound to Langmuir-Blodgett films and self-assembled monolayers. *Mater. Res. Soc. Abstr.* V9.8. (Abstr.)
12. Louie, G. V., W. L. B. Hutcheon, and G. D. Brajer. 1988. Yeast Iso-1-cytochrome c: a 2.8 Å resolution three-dimensional structure determination. *J. Mol. Biol.* 199:295–314.
13. Sagiv, J. 1980. Organized monolayers by adsorption. I. Formation and structure of oleophobic mixed monolayers on solid surfaces. *J. Am. Chem. Soc.* 102:92–98.
14. Ganog, B. R., and R. M. Bell. 1984. Transmembrane movement of phosphatidylglycerol and diacylglycerol sulfhydryl analogues. *Biochemistry.* 23:4977–4983.

15. Bligh, E. G., and W. J. Dyer. 1959. A rapid method of total lipid extraction and purification. *Can. J. Biochem. Physiol.* 37:911–917.

16. Alegria, G. 1989. Use of the Langmuir-Blodgett film technique in structural and functional studies of photosynthetic bacteria. Ph.D. thesis. University of Pennsylvania, Philadelphia, PA.

17. Vanderkooi, J. M., R. Landesberg, G. W. Hayden, and C. S. Owens. 1977. Metal-free and metal-substituted cytochromes *c:* use in characterization of cytochrome *c* binding sites. *Eur. J. Biochem.* 81:339–347.

18. Bill, K., R. P. Casey, B. Clemens, and A. Azzi. 1980. Affinity chromatography purification of cytochrome *c* oxidase. *FEBS (Fed. Eur. Biochem. Soc.) Lett.* 120:248–250.

19. Cherry, R. J., K. Hsu, and D. Chapman. 1972. Polarized absorption spectroscopy of chlorophyll-lipid membranes. *Biochim. Biophys. Acta.* 267:512–525.

20. Blasie, J. K., M. Erecinska, S. Samuels, and J. S. Leigh. 1978. The structure of a cytochrome oxidase-lipid model membrane. *Biochim. Biophys. Acta.* 501:33–52.

21. Tanaka, N., T. Yamani, T. Tsukihara, T. Ashida, and M. Kakudo. 1975. The crystal structure of bonito ferricytochrome *c* at 2.3 Å resolution. *J. Biochem.* (*Tokyo*). 77:147–158.

22. Salemme, F. R., S. T. Freer, N. H. Xuong, R. A. Alden, and J. Kraut. 1973. The structure of oxidized cytochrome c_2 of *Rhodospirillum rubrum. J. Biol. Chem.* 248:3910–3921.

23. Warwicker, J. 1989. Investigating protein-protein interaction surfaces using a reduced stereochemical and electrostatic model. *J. Mol. Biol.* 206:381–395.

24. Moser, C. C., and P. L. Dutton. 1988. Cytochrome *c* and c_2 binding dynamics and electron transfer with photosynthetic reaction center protein and other integral membrane redox proteins. *Biochemistry.* 27:2450–2461.